THE JOURNAL OF BIOLOGICAL CHEMISTRY VOL. 288, NO. 35, pp. 25512–25521, August 30, 2013

Autoxidation and Oxygen Binding Properties of Recombinant Hemoglobins with Substitutions at the αVal-62 or βVal-67 Position of the Distal Heme Pocket*

Received for publication, April 11, 2013, and in revised form, July 18, 2013 Published, JBC Papers in Press, July 18, 2013, DOI 10.1074/jbc.M113.474841

Ming F. Tam, Natalie W. Rice, David H. Maillett, Virgil Simplaceanu, Nancy T. Ho, Tsuey Chyi S. Tam, Tong-Jian Shen, and Chien Ho[1]

From the Department of Biological Sciences, Carnegie Mellon University, Pittsburgh, Pennsylvania 15213

Background: Tertiary structure of the ligand binding pocket influences oxygen binding and autoxidation of hemoglobin.
Results: E11 mutants have increased autoxidation rate. βE11Phe increases, whereas βE11Ile decreases the oxygen binding affinity of hemoglobin.
Conclusion: Bulky residues at βE11 affect ligand binding and cause noticeable tertiary structural changes at the heme pockets.
Significance: Hemoglobin distal heme pocket mutations alter oxygen binding properties without changing the quaternary structure.

The E11 valine in the distal heme pocket of either the α- or β-subunit of human adult hemoglobin (Hb A) was replaced by leucine, isoleucine, or phenylalanine. Recombinant proteins were expressed in *Escherichia coli* and purified for structural and functional studies. ^{1}H NMR spectra were obtained for the CO and deoxy forms of Hb A and the mutants. The mutations did not disturb the $\alpha_1\beta_2$ interface in either form, whereas the H-bond between αHis-103 and βGln-131 in the $\alpha_1\beta_1$ interfaces of the deoxy α-subunit mutants was weakened. Localized structural changes in the mutated heme pocket were detected for the CO form of recombinant Hb (rHb) (αV62F), rHb (βV67I), and rHb (βV67F) compared with Hb A. In the deoxy form the proximal histidyl residue in the β-subunit of rHb (βV67F) has been altered. Furthermore, the interactions between the porphyrin ring and heme pocket residues have been perturbed in rHb (αV62I), rHb (αV62F), and rHb (βV67F). Functionally, the oxygen binding affinity (P_{50}), cooperativity (n_{50}), and the alkaline Bohr Effect of the three α-subunit mutants and rHb (βV67L) are similar to those of Hb A. rHb (βV67I) and rHb (βV67F) exhibit low and high oxygen affinity, respectively. rHb (βV67F) has P_{50} values lower that those reported for rHb (αL29F), a B10 mutant studied previously in our laboratory (Wiltrout, M. E., Giovannelli, J. L., Simplaceanu, V., Lukin, J. A., Ho, N. T., and Ho, C. (2005) *Biochemistry* 44, 7207–7217). These E11 mutations do not slow down the autoxidation and azide-induced oxidation rates of the recombinant proteins. Results from this study provide new insights into the roles of E11 mutants in the structure-function relationship in hemoglobin.

Hemoglobin (Hb)[2] is a tetrameric molecule assuming a $\alpha_2\beta_2$ quaternary structure. Each subunit is densely packed and interacts extensively with a heme molecule that is covalently bound to the proximal histidyl (F8His) residue (1). Hb tetramers reversibly and cooperatively bind oxygen molecules via the ferrous (Fe^{+2}) form of the heme iron atoms. The bound O_2 is further stabilized by hydrogen bonding with the distal histidine E7 (2). Two other residues in the distal heme pocket, B10Leu (αLeu-29 or βLeu-28) and E11Val (αVal-62 or βVal-67), are in close proximity to the ligand binding site (Fig. 1). The importance of these residues on ligand binding has been studied by several groups (3–15).

Autoxidation occurs when the heme-iron atom is oxidized from the ferrous (Fe^{+2}) to the ferric (Fe^{+3}) state with release of superoxide (O_2^-) or perhydroxy (HO_2^-) radical (16). The reaction proceeds with a combination of two mechanisms depending on the concentration of oxygen (O_2) (4). The biological importance of autoxidation is that H_2O_2 can be produced by dismutation of superoxide and leads to both oxidative stress and reactive oxygen species generation. In addition, the resulting Fe^{+3} on hemoglobin cannot bind O_2. Therefore, Hb A is physiologically inactivated when all four iron atoms of the tetramer are oxidized to form methemoglobin (met-Hb). This reaction carries on without catalysis and occurs naturally in normal red blood cells. This process can be promoted by anions (17) and nitric oxide (NO) (6). In erythrocytes, an enzymatic reducing system reverses oxidation of human hemoglobin (Hb A) to met-Hb (18). However, in cell-free solutions the autoxidation reaction leads to more rapid rates of hemin loss resulting in denaturation of the apoglobin (19).

It has long been recognized that Hb can potentially formulate into a substitute for red blood cell transfusion termed hemoglobin-based oxygen carriers (20). However, acellular hemoglobin

* This work was supported, in whole or in part, by National Institutes of Health Grants HL-024525 and GM-0846140. This work was also supported by The Arnold and Mabel Beckman Foundation and the Howard Hughes Medical Institute.

[1] To whom correspondence should be addressed: Dept. of Biological Sciences, Carnegie Mellon University, 4400 Fifth Ave., Pittsburgh, PA 15213. Tel.: 412-268-3395; Fax: 412-268-7083; E-mail: chienho@andrew.cmu.edu.

[2] The abbreviations used are: Hb, hemoglobin; Hb A, human adult Hb; rHb, recombinant Hb; met-Hb, methemoglobin; P_{50}, partial O_2 pressure at 50% saturation; n_{50}, Hill coefficient at 50% O_2 saturation; DSS, 2,2-dimethyl-2-silapentane-5-sulfonate; k_{auto}, autoxidation rate; k_{az}, azide-induced oxidation rate.

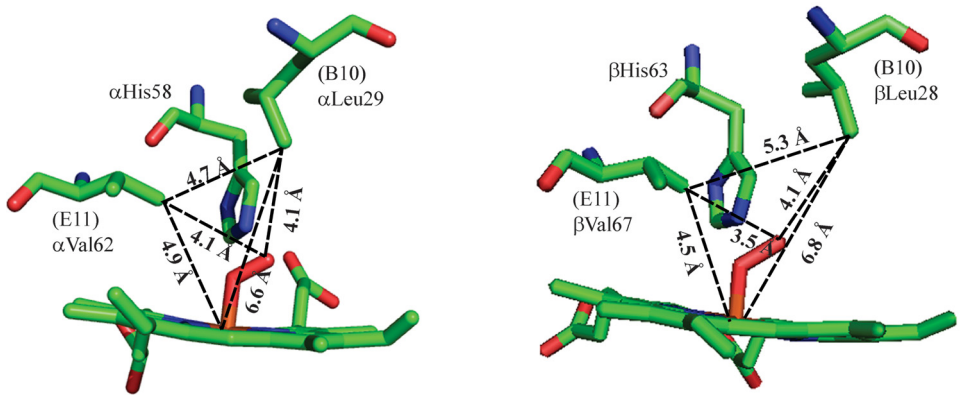

FIGURE 1. **Illustration of the hemoglobin distal heme pockets.** The distances among the iron atom of the heme group, the Val E11 C_{γ}, the Leu B10 C_{γ}, and the bound dioxygen atoms are labeled for the α- (*A*) and β- (*B*) subunits of the oxy-Hb A. Diagrams are generated with the PyMOL program, and coordinates were obtained from PDB entry 2DN1 (57).

diluted into blood dissociates into dimers with subsequent loss in the cooperative oxygenation properties (21) and reacts with endothelium-derived NO with consequent smooth muscle dystonia and clotting disorders (22). Hemoglobins have been cross-linked (23) and polymerized (24) into larger molecules to counteract these effects and achieved mixed results in clinical trials (25, 26). Further improvements can potentially be made by producing "designer" hemoglobin with unique oxygen binding and autoxidation properties.

With the advent of protein engineering, recombinant hemoglobin (rHb) (27–30) with unique properties can be prepared in sufficient quantity for hemoglobin-based oxygen carrier studies. We and others have previously generated B10Leu mutants and shown that replacement of the αB10Leu residue (αLeu-29) with phenylalanine increases the oxygen affinity and decreases the autoxidation rate of the macromolecule (6, 13, 15, 31, 32). We have also produced an octameric hemoglobin with wild type biological activities by substituting the α-subunit Asn-78 residue with cysteine (33). Combination of these mutations produced octameric macromolecules with unique properties that were utilized as resuscitation solutions in mice suffering traumatic brain injury combined with hemorrhagic shock. We observed that the high oxygen affinity rHb (αN78C/L29F) conferred a neuroprotective effect in the selectively vulnerable region of the hippocampus (34).

In light of our success in utilizing rHb as a resuscitation fluid, we have renewed our effort in identifying rHb mutants possessing unique properties for biomedical applications. We report here the characterization of six E11Val mutants. By replacing the βVal-67 with phenylalanine, we have generated a mutant with oxygen affinity even higher than that of rHb (αL29F). Our results affirm the notion that heme pocket mutations can produce macromolecules with unique oxygen binding properties without changing the quaternary structure of hemoglobin.

EXPERIMENTAL PROCEDURES

Materials—Human normal blood samples were obtained from the local blood bank, and Hb A was isolated according to Russu *et al.* (35). Restriction enzymes and related enzymes needed for DNA work were products of New England Biolabs. The QuikChange site-directed mutagenesis kit was purchased from Stratagene. Reagent grade chemicals were obtained from Sigma.

Recombinant Proteins Expression and Purification—The construction of the expression plasmid (pHE2) encoding the *Escherichia coli* methionine aminopeptidase and synthetic human α- and β-globin genes has been reported (29). This plasmid was used as a template with appropriate primers in polymerase chain reactions to replace the αVal-62 or the βVal-67 with leucine, isoleucine, or phenylalanine. The resulting pHE2078, pHE2081, pHE288, pHE2080, pHE2079, and pHE289 plasmids were used for the expression of rHb (αV62L), rHb (αV62I), rHb (αV62F), rHb (βV67L), rHb (βV67I), and rHb (βV67F), respectively. All mutations were confirmed by DNA sequencing.

E. coli JM109 was used as the host for protein expression. The cell culturing and induction conditions and the purification procedure under CO atmosphere have been described by Shen *et al.* (29, 30). The purified proteins were subjected to Edman degradation to estimate the amount of N-terminal methionine cleavage, and the molecular weights of the rHb subunits were confirmed by mass spectrometry in an ion trap instrument equipped with an electrospray ionization source (29). All rHb samples in this study had the correct molecular weights and <5% of N-terminal methionine.

Oxygen Binding Properties—Oxygen dissociation curves were measured using a Hemox Analyzer (TCS Medical Products) as previously described (29). Samples were prepared with 0.1 mM Hb (in terms of heme) in 0.1 M sodium phosphate buffer. Catalase and superoxide dismutase were added to the sample to prevent and/or slow down the formation of met-Hb (36). Experiments were conducted at 29 °C as a function of pH. Oxygen affinity and cooperativity were determined for each sample from the resulting oxygen equilibrium curves. To analyze the results, the equilibrium binding curves were fit to the Adair equation using a nonlinear least-squares procedure. The oxygen affinity of the sample was determined from the P_{50} value (in millimeters of Hg). To measure cooperativity, values for n_{50} (the Hill coefficient) were calculated from the slope of the Hill

plot at 50% saturation. The values had an accuracy of ±10%. Experimental results have S.D. ± 4% between runs.

Structural Study with ^{1}H NMR Spectroscopy—Proton spectra of Hb A and rHbs in CO or the deoxy form were collected on Bruker Avance DRX-300 or DRX-600 spectrometers. Hb samples were exchanged into 0.1 M sodium phosphate, pH 7.0, and concentrated to an ~5% (3.1 mM in terms of heme) solution. Deuterium oxide was then added to a final concentration of 5%, and measurements were made at 29 °C. A jump-and-return pulse sequence was used to suppress the water signal (37). The methyl proton resonance (4.76 ppm upfield of the water signal at 29 °C) of 2,2-dimethyl-2-silapentene-5-sulfonate (DSS) was used as internal reference for the proton chemical shifts.

Autoxidation of Hb A and rHbs—Autoxidation of hemoglobin samples was measured according to Wiltrout *et al.* (15). Briefly, concentrated rHbs stored in CO form were oxygenated under a constant stream of 100% O_2 in a rotary evaporator for a 1 h minimum under lamp light and in an ice bath. The $rHbO_2$ was then diluted immediately to 60 μM in terms of heme (A_{577} ~ 1.0) with 0.1 M sodium phosphate, pH 7.0, and 1 mM EDTA. The samples were then transferred without delay into capped cuvettes and a temperature-controlled holder at 25 °C in a Cary 50 UV-visible spectrophotometer (Varian). Absorbances at 560, 577, 630, and 700 nm were recorded every 15 min for 7 h. The optical density readings at 700 nm were normally less than 0.02 at the end of data acquisition and used to assure the lack of sample precipitation during the time of data acquisition. They were treated as background readings and subtracted from the readings of the other three wavelengths. The major components in the reaction mixtures were oxy-Hb, met-Hb, and hemichrome, and their respective concentrations can be calculated from these absorbances and their extinction coefficients determined at the corresponding wavelengths (38). The millimolar extinction coefficients ($mM^{-1}\ cm^{-1}$) for oxy-Hb and met-Hb at pH 7.0 have been reported by Benesch *et al.* (38) on per heme base, and they are: $\epsilon_{560} = 9.06$, $\epsilon_{577} = 16.5$, and $\epsilon_{630} = 0.15$ for oxy-Hb; $\epsilon_{560} = 4.05$, $\epsilon_{577} = 4.06$, and $\epsilon_{630} = 4.01$ for met-Hb. The millimolar extinction coefficients ($mM^{-1}\ cm^{-1}$) per heme base for hemichrome were calculated from those reported originally by Winterbourn *et al.* (39) per tetramer base. Numerically they are: $\epsilon_{560} = 9.13$, $\epsilon_{577} = 7.15$ and $\epsilon_{630} = 0.975$. The following simultaneous equations can then be written,

$$A_{560} = 9.06\,[\text{oxy-Hb}] + 4.05\,[\text{met-Hb}] + 9.13\,[\text{hemichrome}] \quad \text{(Eq. 1)}$$

$$A_{577} = 16.5\,[\text{oxy-Hb}] + 4.06\,[\text{met-Hb}] + 7.15\,[\text{hemichrome}] \quad \text{(Eq. 2)}$$

$$A_{630} = 0.15\,[\text{oxy-Hb}] + 4.01\,[\text{met-Hb}] + 9.75\,[\text{hemichrome}] \quad \text{(Eq. 3)}$$

After rearranging, $[\text{oxy-Hb}] = -0.0786A_{560} + 0.1041A_{577} - 0.0259A_{630}$. The concentration of oxy-Hb at each time point can then be calculated and expressed as percent of the original sample. The logarithm (base 10) of percent oxy-Hb was then plotted as a function of time, and the slope of the plot gives the first-order rate constant of autoxidation.

Samples were prepared similarly for azide-induced oxidation experiments except that the reaction mixture had an additional 0.1 M sodium azide. Absorbances were measured at 577, 630, and 700 nm every 15 min for 7 h. Readings at 700 nm were used for base-line subtractions and indicators for protein precipitation. The millimolar extinctions coefficients ($mM^{-1}\ cm^{-1}$) for azidomet were those reported by Jeong *et al.* (13), and they are $\epsilon_{577} = 8.37$ and $\epsilon_{630} = 1.98$ after converting into per heme base. Calculations were treated as above, and the final equation for determining the concentration of oxy-Hb has the form of $0.063A_{577} - 0.2664A_{630}$. For some rHb mutants, precipitation occurred 5 h after adding azide. Therefore, only data collected for the first 4 h were used in calculations.

RESULTS

Oxygen Binding Properties—The O_2 binding properties of Hb A and the six rHb with substitutions at the E11 position, rHb (αV62L), rHb (αV62I), rHb (αV62F), rHb (βV67L), rHb (βV67I), and rHb (βV67F), are presented in Fig. 2. Data for rHb (αL29F) (15), a high O_2 affinity B10 mutant, were included for comparison. Fig. 2*A* demonstrates clearly that the replacement of the α-subunit E11Val with leucine, isoleucine, or phenylalanine has not significantly changed the O_2 binding properties of the macromolecule. Similarly, rHb (βV67L) is functionally nearly identical to Hb A. The rHb (βV67I) mutant, however, has low O_2 binding affinity. Interestingly, by placing an aromatic residue at the E11 position of the β-subunit, we generated a high O_2 affinity mutant in rHb (βV67F). This mutant has higher oxygen affinity than that reported for rHb (αL29F) (13, 15).

The Hill coefficients (n_{50}), an indicator of cooperativity in the oxygenation process of Hb, are plotted as a function of pH in Fig. 2*B*. All mutants investigated cooperatively bind oxygen. rHb (αV62I) and rHb (αV62L) exhibited a high level of cooperativity, comparable to Hb A, whereas other distal heme pocket mutants in this study exhibited noticeable decreases in the Hill coefficient. As summarized in Table 1, the Hill coefficients at pH 7.4 for Hb A, rHb (αV62L), rHb (αV62I), rHb (αV62F), rHb (βV67L), rHb (βV67I), and rHb (βV67F), are 2.8, 2.8, 3.0, 2.4, 2.7, 2.5 and 2.0. In particular, the rHb (βV67F) mutant has Hill coefficients between 1.5 and 2.3 within the pH range of 5.7–8.2. These values are significantly lower than those of Hb A but indicate that the mutant still maintains a low level of cooperativity.

The affinity between oxygen and Hb decreases upon lowering the pH of the solution. This alkaline Bohr Effect can be estimated from the slope of the log P_{50} *versus* pH plot, and the values for Hb A and the six E11 mutants are listed in Table 1. With the exception of rHb (βV67F), all other proteins on the list have a calculated value of 0.45–0.48. The lower Bohr Effect (0.36) observed for rHb (βV67F) implies that the mutant has a smaller change in oxygen affinity upon lowering pH. Consequently, less oxygen could be released in muscle capillaries with high levels of lactic acid.

Autoxidation and Azide-induced Oxidation—The autoxidation rates of Hb A and mutants were measured in 0.1 M sodium

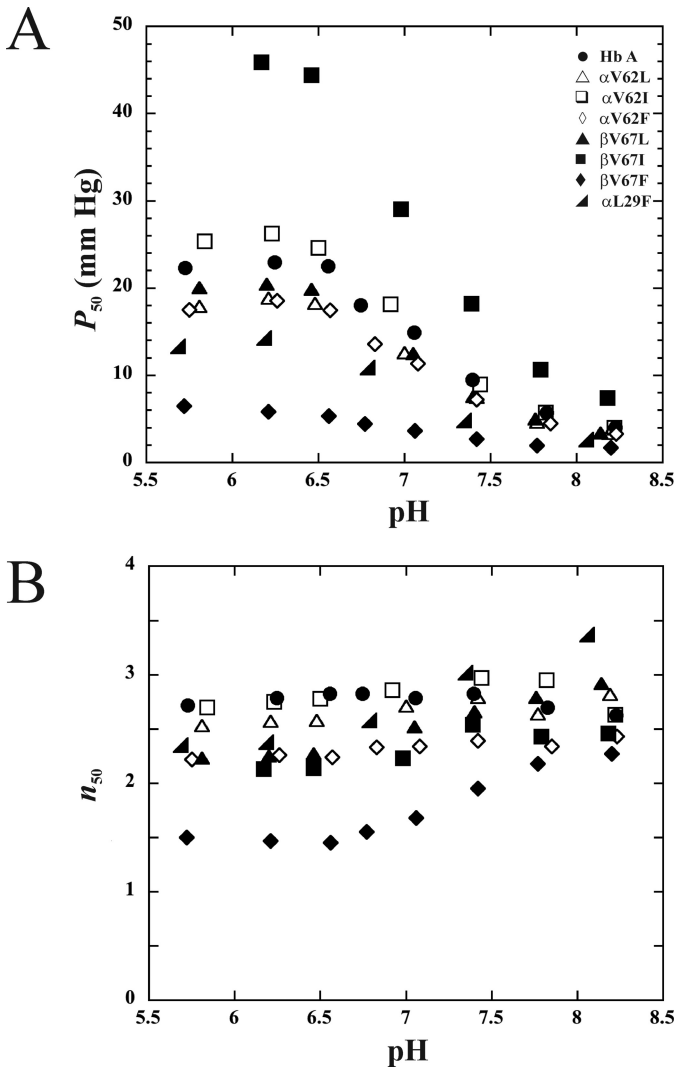

FIGURE 2. **Oxygen binding properties of Hb A and rHbs.** Data were acquired in 0.1 M sodium phosphate at 29 °C. The oxygen affinities (*A*) and Hill coefficients (*B*) are plotted as a function of pH.

phosphate at pH 7.0 and 25 °C. Data were acquired for 7 h and treated as a mono-exponential process according to Wiltrout *et al.* (15). The results represent the initial autoxidation rates, and the rate constants, k_{auto}, as summarized in Table 2, are the average rate constants for the first 7 h of the reactions. Under the experimental conditions employed, HbO_2 A has an autoxidation rate constant of 7.8×10^{-4} h^{-1}. All E11 mutants in this study have higher k_{auto} values than that of Hb A. The values obtained range from 3.2-fold higher for rHb (αV62I) to 7-fold higher for rHb (βV67F).

Azide anions form stable complexes with oxidized iron (Fe^{3+}). Hemoglobins can be converted into the azidomet form with sodium azide (13, 40). The heme irons can then undergo further conversions to soluble and insoluble hemichromes (19). In the presence of 0.1 M sodium azide, rHb (αV62L), rHb (αV62F), rHb (βV67L), and rHb (βV67F) form precipitates after incubating at pH 7.0 and 25 °C for 5 h. Therefore, the azide-induced oxidation rates (k_{az}) for Hb A and the mutants were calculated for the first 4 h of reaction and listed in Table 2. Not surprisingly, stable proteins such as rHb (αV62I) and rHb (βV67I) have k_{az} values close to that of Hb A. The k_{az} for rHb (αV62L), rHb (βV67L), rHb (αV62F), and rHb (βV67F) are 2.3-, 2.5-, 3.0-, and 3.6-fold higher than that of Hb A, respectively (Table 2). None of the E11 mutants tested inhibited azide-induced oxidation as did rHb (αL29F).

Structural Properties—^{1}H NMR has been used routinely to probe tertiary and quaternary structural changes in hemoglobin (41). The E11 mutants generated for this study in CO (Fig. 3) and deoxy (Fig. 4) forms were analyzed with this technique in 0.1 M sodium phosphate buffer at pH 7.0 and 29 °C.

NMR Spectra of Hemoglobins in CO Form—Fig. 3 shows the ^{1}H NMR spectra for Hb A and rHbs in the CO form. Resonance signals between 9 and 14 ppm have been assigned to the exchangeable protons in the intersubunit interfaces. The resonances at 12.9 and 12.1 ppm have been assigned to the $NH_{\epsilon 1}$ of the side chains of αHis-122 and αHis-103, respectively (42–44). These two histidines are located within the $\alpha_1\beta_1$ interface. The resonance at 10.6 ppm has been assigned to the $NH_{\epsilon 1}$ of βTrp-37 (44, 45), which is an $\alpha_1\beta_2$ interface residue. No change in the chemical shift for these resonances was observed for all six E11 rHbs in relation to Hb A (Fig. 3*A*), indicating no perturbation to their quaternary structure at the $\alpha_1\beta_1$ and $\alpha_1\beta_2$ interfaces.

We observed marked changes in the resonances in the region between 9.5 and 10.5 ppm. In particular, an additional peak at ~9.8 ppm can be observed for the 2 mutants with aromatic amino acid substitution. However, we do not have resonance assignments for these signals, and we cannot elaborate on the origins of these disturbances.

Resonances from 0 to −3 ppm belong to the non-exchangeable ring current-shifted protons and provide information about the tertiary structure of the heme pockets. The signals at −1.75 and −1.82 ppm relative to DSS have been assigned to the γ_2-CH_3 group of αVal-62 and βVal-67, respectively (46, 47). For the α-subunit E11 mutations, the resonance corresponding to αVal-62 is absent from the spectra. Likewise, the resonance for the βVal-67 is absent from the spectra for the β-subunit mutations. For the βV67L and βV67F mutants, the resonances between −0.5 to −1.1 ppm differ significantly from those of HbCO A, but we have not yet assigned the resonances for these signals.

Combining these observations, we conclude that the mutants in the liganded form maintain their quaternary structure. Localized structural changes in the mutated heme pocket have been detected for rHb (αV62F), rHb (βV67I), and rHb (βV67F).

NMR Spectra of Hemoglobins in Deoxy Form—Fig. 4 shows the ^{1}H NMR spectra for Hb A and rHbs in the deoxy form. The hyperfine-shifted proton resonances of the $N_\delta H$ exchangeable proton of proximal histidines are between 60 and 80 ppm from DSS. The resonances at 63 and 76 ppm have been assigned to αHis-87 and βHis-92 of the deoxy Hb A (48, 49), respectively. For the three α-subunit E11 mutants, the resonance at 76 ppm remains unchanged. However, the signal at 63 ppm has shifted 1.5–2.5 ppm downfield (Fig. 4*A*). The results suggest that these α-subunit mutations slightly disturb the tertiary structure of the proximal heme pockets in the mutated subunits. Among the three β-subunit mutants, only rHb (βV67F) displays a

TABLE 1

Oxygen binding properties and Bohr Effect of Hb A and recombinant mutants

Experiments were conducted in 0.1 M sodium phosphate buffer at 29 °C in the presence of a methemoglobin reductase system (36). Values for Bohr Effect were estimated from the pH range in parentheses. Experimental results have S.D. ± 4% between runs.

Hemoglobins	pH	P_{50}	n_{50}	$-\Delta(\log P_{50})/\Delta pH$	Hemoglobins	pH	P_{50}	n_{50}	$-\Delta(\log P_{50})/\Delta pH$
Hb A	5.73	22.22	2.71	0.46 (pH 6.56–8.23)	rHb (βV67L)	5.81	20.03	2.23	0.47 (pH 6.46–8.14)
	6.25	22.86	2.78			6.20	20.44	2.25	
	6.56	22.44	2.82			6.46	19.86	2.27	
	6.75	17.97	2.82			7.05	12.49	2.52	
	7.06	14.80	2.78			7.40	7.53	2.66	
	7.40	9.38	2.82			7.76	4.97	2.79	
	7.83	5.61	2.69			8.14	3.37	2.92	
	8.23	3.93	2.62		rHb (βV67I)	6.17	45.86	2.13	0.47 (pH 6.46–8.18)
rHb (αV62L)	5.81	17.88	2.53	0.45 (pH 6.48–8.19)		6.46	44.40	2.14	
	6.21	18.84	2.57			6.98	29.01	2.23	
	6.48	18.23	2.58			7.39	18.17	2.54	
	7.00	12.55	2.71			7.79	10.65	2.43	
	7.42	7.48	2.79			8.18	7.41	2.46	
	7.77	4.64	2.64		rHb (βV67F)	5.72	6.48	1.50	0.36 (pH 6.56−7.77)
	8.19	3.32	2.82			6.21	5.82	1.47	
rHb (αV62I)	5.84	25.34	2.70	0.48 (pH 6.50–8.22)		6.56	5.33	1.45	
	6.23	26.24	2.75			6.77	4.41	1.55	
	6.50	24.60	2.78			7.06	3.65	1.68	
	6.92	18.14	2.86			7.42	2.67	1.95	
	7.44	8.97	2.97			7.77	1.94	2.18	
	7.82	5.70	2.95			8.20	1.68	2.27	
	8.22	3.99	2.63		rHb (αL29F)[a]	6.20	14.27	2.38	0.46 (pH 6.20–8.07)
rHb (αV62F)	5.75	17.52	2.22	0.45 (pH 6.57–8.23)		6.80	10.87	2.58	
	6.26	18.54	2.26			7.36	4.84	3.02	
	6.57	17.44	2.24			8.07	2.62	3.37	
	6.83	13.58	2.33						
	7.08	11.35	2.34						
	7.42	7.19	2.39						
	7.85	4.48	2.34						
	8.23	3.29	2.43						

[a] Data were from Wiltrout *et al.* (15).

TABLE 2

Autoxidation and azide-induced apparent oxidation rate constants of Hb A and recombinant mutants

Data were acquired in 0.1 M sodium phosphate, pH 7.0, and 1 mM EDTA at 25 °C. Each value represents the mean ± S.D. from two preparations of triplicate samples.

Hemoglobins	k_{auto}[a]	k_{az}[b]
	h^{-1}	h^{-1}
Hb A	0.0008 ± 0.0002	0.071 ± 0.007
rHb (αV62L)	0.0037 ± 0.0001	0.165 ± 0.022
rHb (αV62I)	0.0025 ± 0.0002	0.064 ± 0.009
rHb (αV62F)	0.0044 ± 0.0001	0.210 ± 0.010
rHb (βV67L)	0.0035 ± 0.0001	0.175 ± 0.008
rHb (βV67I)	0.0030 ± 0.0002	0.094 ± 0.003
rHb (βV67F)	0.0054 ± 0.0004	0.259 ± 0.005
rHb (αL29F)[c]	0.0009 ± 0.0002	0.014 ± 0.002

[a] k_{auto}, autoxidation rate.
[b] k_{az}, azide-induced oxidation rate.
[c] Data were from Wiltrout *et al.* (15).

spectrum that differs from that of Hb A in this region. The resonance at 63 ppm remains unchanged, whereas the signal at 76 ppm broadened and shifted 3.5 ppm downfield (Fig. 4*A*). The observation is indicative of a structural change in the proximal heme pocket of the β-subunit of rHb (βV67F), and the change is more severe than those observed for the αE11 mutants.

The spectral region between 16–25 ppm downfield from DSS is presented in Fig. 4*B*. The resonances at 17.0 and 22.6 ppm represent signals generated by the porphyrin ring of the α- and β-subunits, respectively (41). The rHb (αV62L), rHb (βV67L), and rHb (βV67I) have a similar NMR pattern in this region as Hb A (Fig. 4*B*). For the rHb (αV62I) and rHb (αV62F) mutants, the signal at 17.0 ppm has shifted 1.5 ppm downfield and upfield, respectively, from its original position. A much larger perturbation in the spectrum has been observed for the rHb (βV67F) mutant. The resonance at 22.6 ppm has shifted ~3 ppm upfield and broadened. All these results are indicative of the local structural disturbances in the heme pocket where the mutation has taken place.

Resonances at 14.1 and 11.2 ppm have been assigned to H-bonds between residues in the $\alpha_1\beta_2$ interface of deoxy Hb A. The resonance at 14.1 ppm represents the H-bond between αTyr-42 and βAsp-99 (50). The resonance at 11.2 ppm denotes the exchangeable NH indole proton of βTrp-37 that H-bonds to αAsp-94. Both of these resonances are important T-state markers of the deoxy-Hb A (44, 50, 51). rHb (αV62I) exhibits a slight chemical shift of 0.3 ppm upfield for the $\alpha_1\beta_2$ interface peaks. Overall, the E11 mutations exhibit little to no perturbation of the $\alpha_1\beta_2$ interface.

As in the CO form, αHis-122 and αHis-103 in the $\alpha_1\beta_1$ interface of deoxy-Hb A give resonance signals at 13.0 and 12.2 ppm from DSS, respectively. Mutants that have substitution at the βE11Val position do not affect the resonances at these positions. However, the αE11 mutants clearly suppress the resonance signal at 12.2 ppm. Apparently, these α-subunit mutations interfere with the H-bond between αHis-103 and βGln-131 (42).

Overall, in the deoxy form the substitutions that we have made at the E11 position have not disturbed the $\alpha_1\beta_2$ interfaces. The α-subunit mutants have a weaker H-bond between αHis-103 and βGln-131, which are $\alpha_1\beta_1$ interface residues. The α-subunit mutations slightly affect the proximal histidyl residue, whereas the βE11Val to phenylalanine replacement creates a more pronounced disturbance on the proximal histidyl residue. In addition, interactions between the porphyrin ring

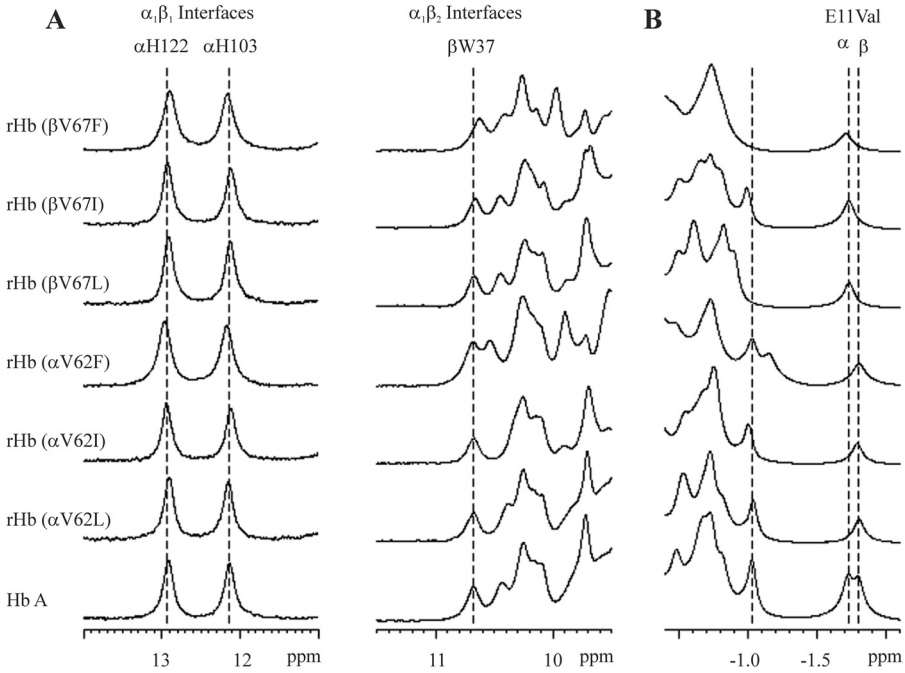

FIGURE 3. **^{1}H NMR spectra of Hb A and rHbs in the CO form.** Data were acquired in 95% H_2O, 5% D_2O, and 0.1 M sodium phosphate buffer at pH 7.0 and 29 °C. Shown are exchangeable proton resonances (*A*) and ring current-shifted proton resonances (*B*).

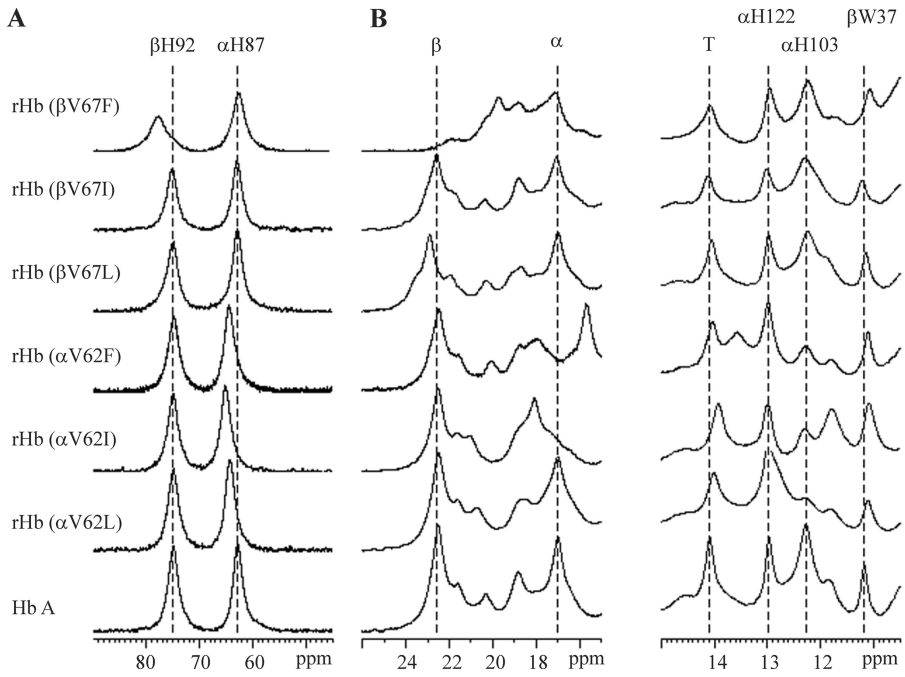

FIGURE 4. **^{1}H NMR spectra of Hb A and rHbs in the deoxy form.** Data were acquired in 95% H_2O, 5% D_2O, and 0.1 M sodium phosphate buffer at pH 7.0 and 29 °C. Shown are hyperfine-shifted $N_\delta H$ proton resonances of proximal histidyl residues (*A*) and hyperfine-shifted and exchangeable proton resonances (*B*).

and heme pocket residues have been perturbed in rHb (αV62I), rHb (αV62F), and rHb (βV67F).

DISCUSSION

Hemoglobin functions as an O_2 carrier and the heme pocket is the ligand binding/active center of the protein. In the center of the cavity are the proximal F8His and the distal E7His. F8His covalently binds the heme onto the protein for O_2 binding, whereas E7His stabilizes the bound O_2 with hydrogen bonds (52, 53) and acts as a gate for ligand entry (52, 54).

Two other important residues within the reaction center are B10Leu and E11Val (Fig. 1). Hemoglobin mutants carrying an aromatic replacement at the B10 position have been characterized by several groups (6, 13, 15, 31, 52, 55). Wiltrout *et al.* (15) substituted B10Leu with either phenylalanine or tryptophan. Among the four mutants, only rHb (αL29F) has a similar autox-

idation rate and a higher O_2 affinity than Hb A (Fig. 2). The other three mutants bind O_2 with low affinity and have higher autoxidation rates than that of the wild type protein (15). In general, the two α-subunit mutants have lower azide- and NO-induced oxidation rates, whereas the two β-subunit mutants have a lower NO-induced but higher azide-induced oxidation rates than Hb A (6, 15). Presumably, an aromatic residue at the B10 position decreased the volume of the distal pocket and creates a steric hindrance that hinders the accessibility of the iron atom to solvent water molecules, NO, and azide anions, resulting in diminished autoxidation and induced oxidation rates. This interpretation is consistent with O_2 and CO binding and CO geminate rebinding studies in rHb(αV1M/L29F, βV1M) and rHb(αV1M/L29W, βV1M) triple mutants (31). In that work placement of the aromatic residues at position B10 was shown to dramatically reduce (i) the fraction of geminate recombination and (ii) association rate constants for ligand binding, demonstrating that the mutations interfere with ligand entry and bond formation in the α-subunit. The phenylalanine substitution further stabilizes the bound oxygen with the positive edge of the phenyl ring multipole and consequently increases the oxygen binding affinity (5). The distal heme pocket of the β-subunit assumes a comparatively more open structure in the R-state (9), and similar B10 substitutions are less effective in lowering the autoxidation rates.

E11Val occupies a unique position in the distal heme pockets. Its methyl γ_2 is 5.2 and 4.2 Å from the iron atom of the porphyrin group of the deoxy Hb A α- and β-subunits, respectively (56). According to the 1.25 Å resolution crystal structural model (PDB ID 2DN1 (57)), the distance between the methyl γ_2 of E11Val and the bound O_2 atom is 4.07 and 3.52 Å in the α- and the β-chains of HbO_2 A, respectively (Fig. 1). Apparently, βE11Val can restrict or interfere with ligand binding, and this restriction is exerted to a lesser extent by αE11Val in the α-subunits.

We have replaced the αVal (E11) with leucine, isoleucine, and phenylalanine in this study. These mutants have similar cooperativity (n_{50}) and alkaline Bohr Effect (Fig. 2 and Table 1) as Hb A. The O_2 binding affinities (P_{50}) of these mutants are also similar to that of Hb A at neutral or basic pH. Under acidic conditions, rHb (αV62L) and rHb (αV62F) have identical O_2 binding curves, and the affinities are slightly higher than that of Hb A. As for the rHb (αV62I) mutant, it exhibits a slightly lower O_2 binding affinity than that of Hb A at acidic pH (Fig. 2). Similar observations have been reported by Mathews *et al.* (10) for the rHb (αV62I) mutant and by Maillett (31) for the rHb(αV1M/L29F, βV1M) mutant.

Leucine has a flexible aliphatic side chain. Replacing αE11Val with leucine causes minimal disturbance to the structure of the macromolecule in the R-state (Fig. 3). In the T-state (Fig. 4*B*), we have detected a weakening of an H-bond (between αHis-103 and βGln-131) located in the $\alpha_1\beta_1$ interfaces, and this phenomenon is common for all three α-subunit mutants. According to the x-ray crystallographic model (57), αVal-62 is >16 Å from αHis-103. The replacements at αE11 probably affect αHis-103 via αHis-87, the proximal histidine. Our hyperfine-shifted protein resonance spectra (Fig. 4*A*) indicate a shift in the αHis-87 signal for these three α-subunit mutants. The main-chain oxygen of αHis-87 forms H-bonds with αArg-92 and αVal-93. These two residues are part of a loop that connects and forms H-bonding network with the αG helix, where αHis-103 is located. It is of interest to note that a αHis-87 to glycine substitution can shift the signal from the $NH_{\epsilon 1}$ of αHis-122 upfield (58). αHis-122 is another residue located in the $\alpha_1\beta_1$ interface and over 22 Å from αHis-87. Further experiments are needed to test our speculation.

Phenylalanine has a bulkier side chain than that of leucine. Consequently, slight changes in the tertiary structure of the heme pocket in the R-state (Fig. 3*B*) and interactions among the porphyrin ring and surrounding amino acids (Fig. 4*B*) have been noticed for rHb (αV62F). However, these structural alterations have not translated into functional changes, and the O_2 binding affinities of rHb (αV62F), rHb (αV62L), and Hb A are similar. These observations are consistent with measurements of O_2 binding to a rHb (αV1M/V62F, βV1M) mutant, which showed that ligand association was promoted by removal of the γ-CH_3 group but countered by steric hindrance to ligand capture, resulting in little impact on O_2 affinity (31). The increase in side-chain volume from leucine to phenylalanine at the αE11 position does not significantly change O_2 binding (Fig. 2*A*) or the azide-induced oxidation (Table 2) rates of the macromolecule.

Tame *et al.* (59) have determined the crystal structures of rHb (αV62L) and rHb (αV62I) in the deoxy state. The extra methyl group of the isoleucine side chain has replaced a water molecule found inside the heme pocket of the α-subunits of hemoglobins. Our ^{1}H NMR analyses indicate that the αE11Val-to-isoleucine substitution causes a change in the porphyrin ring interacting in the T-state of the mutant (Fig. 4*B*). The non-exchangeable ring current-shifted proton spectrum between −0.5 to −1.0 ppm also suggests a slight change in the tertiary structure of the heme pocket of rHb (αV62I) in the R-state. However, none of these structural changes significantly affect the O_2 binding affinity of rHb (αV62I) (Fig. 2*A*).

The presence of the γ-CH_3 group in the α-subunit appears to slightly inhibit azide-induced oxidation. Rate constants measured for Hb A and rHb (αV62I) are similar and lower than those observed for rHb (αV62L) and rHb (αV62F) (Table 2). This result implies that removal of the γ-CH_3 group at position 62 facilitates azide anion access to the iron atom. In contrast, rates of autoxidation were similar in rHb (αV62L), rHb (αV62I), and rHb (αV62F) but still 3.2–5.5-fold higher than that of Hb A (Table 2).

Due to the close proximity of βE11Val to the ligand binding site, a selected mutation at this position can affect the activity of hemoglobin. The crystal structure of deoxy rHb (βV67L) has been resolved at 2.18 Å. The βE11Leu side chain is disordered, and the mutation has caused a small movement in the E-helix (11). Our hyperfine-shifted proton resonance spectrum for the T-state of rHb (βV67L) also indicates a slight shift in the signal that normally appears at 22.6 ppm (Fig. 4*B*). With the disappearance of the signal at −1.0 ppm, the ring-current shift proton resonance spectrum (Fig. 3*B*) suggests a slight structural change in the heme pocket of this mutant at the R-state. These changes do not significantly affect the O_2 binding affinity of rHb (βV67L) (Fig. 2 and Ref. 11). Presumably, due to the flexibility of

the leucine side chain, it is easier for the oxygen and azide anions to access the heme irons. rHb (βV67L) has a higher autoxidation rate and azide-induced oxidation rate than Hb A (Table 2). The situation is analogous to that of Hb Sydney, which has a βE11Val-to-alanine replacement. With a smaller side chain at the βE11 position, Hb Sydney is easily autoxidized and unstable (60).

Like the valine side chain, a branched isoleucine side chain on the E-helix cannot rotate about the C_α-C_β bond, and its δ-methyl group shields the binding site and hinders oxygen binding (11). The conformations of rHb (βV67I) in both T- and R-states are similar to those of Hb A. Among the ^{1}H NMR spectra generated for this mutant, we have detected a missing peak at −1.82 ppm (assigned to the γ_2-CH_3 group of βVal-67) from the ring current shift proton resonance spectrum for the R-state of the mutant. Compared with valine, the bulkier side chain of isoleucine effectively hinders the binding of oxygen and azide anions. Consequently, rHb (βV67I) has a lower binding affinity for O_2 (Fig. 2) and similar azide-induced oxidation rate (Table 2). The autoxidation rate of rHb (βV67I) is only 3.8 times higher than that of Hb A.

Unlike the corresponding α-subunit mutation, placement of a phenylalanine residue at the βE11 position significantly changes the heme pocket of the mutant. Noticeably, in the T-state, the signal at 76 ppm and assigned to the N_δH of βHis92 shifted downfield (Fig. 4*A*), whereas the signal at 22.5 ppm and assigned to the β-subunit porphyrin ring shifted upfield. The spectra for rHb (βV67F) at the R-state are similar to those of Hb A and rHb (βV67L) (Fig. 3). Therefore, the βE11Val to phenylalanine substitution affects the proximal βHis-92 and the interactions between the porphyrin ring and surrounding amino acid residues when the macromolecule assumes the T-state conformation. This substitution does not cause meaningful structural changes to the protein in the R-state conformation.

The structure of rHb (βV67F) has not been elucidated. However, an x-ray crystallographic model for the corresponding myoglobin mutant (V68F) is available (61). The benzyl side chain of the myoglobin mutant points away from the ligand binding site and packs at the back of the distal pocket. Consequently, the heme iron is more readily accessible for ligand binding than that of the myoglobin βV67L and βV67I mutants. Presumably, the βPhe-67 side chain on rHb (βV67F) can assume a similar conformation and its preference to stay in the R-state, resulting in a drastic increase in oxygen binding affinity (Fig. 2).

Studies of geminate recombination, O_2 equilibrium binding, and ligand association and dissociation reactions are consistent with this interpretation (31). In that work, rHb (αV1M, βV1M/V62F) was shown to have decreased rates of O_2 association due to steric hindrance of the bulky aromatic ring, but this effect was more than counteracted by a marked decrease in O_2 dissociation rates attributed to removal of the γCH_3 group, resulting in a substantial increase in O_2 affinity. Fitting of the equilibrium binding curve to a two-state model indicated a decrease in the R ↔ T equilibrium constant (L), suggesting a possible structural mechanism consistent with the observations made in this work.

Even though phenylalanine has a bulky aromatic side chain and is expected to effectively decrease the distal pocket volume, it is not as effective as the methyl γ_2 of the native valine side chain in protecting the iron atom of the heme. The k_{az} of rHb (βV67F) is 3.6-fold higher than that of Hb A. The autoxidation rate of rHb (βV67F) is 7-fold higher than that of Hb A and comparable to that of rHb (αL29W) (15). Eich *et al.* (6) determined the NO-induced oxidation rate of rHb (βV67F) in the R-state, and it is 4.5-fold slower than that of Hb A. The higher azide-induced (this work) and lower NO-induced (6) oxidation rates of rHb (βV67F) compared with those of Hb A illustrate differences in the mechanisms of these oxidation reactions. NO-induced oxidation depends upon the rate of NO entry into the pocket, whereas azide-induced oxidation occurs on a slower time frame and is dependent upon the affinity for azide. In rHb (βV67F), the presence of the aromatic group in the ligand binding pocket interferes with ligand entry, slowing NO-induced oxidation, but removal of the γCH_3 group may increase azide affinity, explaining the increase in azide-induced oxidation based on the findings from the myoglobin study (62). This interpretation is consistent with CO bimolecular binding, and geminate rebinding results in Hb(αV1M, βV1M/V62F) mutant that found k'_{entry} was reduced by the aromatic substitution (31). A more detailed structural model of rHb (βV67F) is needed to delineate whether and how additional residues located in the heme pockets participate in the mechanism. It is reasonable to postulate that the tertiary structure of the distal heme-pocket is of primary importance in determining rates of autoxidation and ligand binding. However, the differential stability of the Hb mutants in their R- and T-states contributes to the oxygen affinity of the proteins.

We have recently employed recombinant octameric hemoglobins carrying αB10Leu to phenylalanine or tryptophan replacements as resuscitation solutions in mice after experimental traumatic brain injury plus hemorrhagic shock (34). Both mutants have reduced rates of NO-induced oxidation. However, the αL29F mutant has high, whereas the αL29W mutant has low O_2 binding affinity (15). We have found that the high O_2 affinity αL29F mutant has the lowest numerical brain tissue oxygen concentration and unexpectedly a better neuronal survival (34). Interestingly, Eaton *et al.* (63) have reported that Hb with higher O_2 affinity gave better protection to animals placed at greatly reduced environmental oxygen pressures. Deer mice adapted to high altitude also carry Hb isoforms with higher intrinsic O_2 affinities (64). Furthermore, Cole *et al.* (65) proposed a mathematical model for O_2 transport and postulated that cell-free oxygen carriers should have P_{50} in the range of 5–15 mm Hg, which is higher or equivalent to that of Hb A. The rHb (βV67F) in this study has an O_2 binding affinity higher than that of the αL29F mutant (Fig. 2), and it has reduced NO-induced oxidation rate (6). Thus, our work here has further advanced the understanding of the structure-function relationship of hemoglobin. Incidentally, it also provides a candidate (rHb (βV67F)) to be used in resuscitation solutions and can be tested in a mouse model representing traumatic brain injury combined with hemorrhagic shock.

Acknowledgment—We thank Dr. Yue Yuan for helpful discussions and technical guidance.

REFERENCES

1. Dickerson, R. E., and Geis, I. (1983) *Hemoglobin: Structure, Function, Evolution, and Pathology*, pp. 26–47, Benjamin/Cummings, Menlo Park, CA
2. Lukin, J. A., Simplaceanu, V., Zou, M., Ho, N. T., and Ho, C. (2000) NMR reveals hydrogen bonds between oxygen and distal histidines in oxyhemoglobin. *Proc. Natl. Acad. Sci. U.S.A.* **97,** 10354–10358
3. Birukou, I., Maillett, D. H., Birukova, A., and Olson, J. S. (2011) Modulating distal cavities in the α and β subunits of human HbA reveals the primary ligand migration pathway. *Biochemistry* **50,** 7361–7374
4. Brantley, R. E., Jr., Smerdon, S. J., Wilkinson, A. J., Singleton, E. W., and Olson, J. S. (1993) The mechanism of autooxidation of myoglobin. *J. Biol. Chem.* **268,** 6995–7010
5. Carver, T. E., Brantley, R. E., Jr., Singleton, E. W., Arduini, R. M., Quillin, M. L., Phillips, G. N., Jr., and Olson, J. S. (1992) A novel site-directed mutant of myoglobin with an unusually high O_2 affinity and low autooxidation rate. *J. Biol. Chem.* **267,** 14443–14450
6. Eich, R. F., Li, T., Lemon, D. D., Doherty, D. H., Curry, S. R., Aitken, J. F., Mathews, A. J., Johnson, K. A., Smith, R. D., Phillips, G. N., Jr., and Olson, J. S. (1996) Mechanism of NO-induced oxidation of myoglobin and hemoglobin. *Biochemistry* **35,** 6976–6983
7. Fronticelli, C., Brinigar, W. S., Olson, J. S., Bucci, E., Gryczynski, Z., O'Donnell, J. K., and Kowalczyk, J. (1993) Recombinant human hemoglobin. Modification of the polarity of the β-heme pocket by a valine 67(Glu-11) → threonine mutation. *Biochemistry* **32,** 1235–1242
8. Karavitis, M., Fronticelli, C., Brinigar, W. S., Vasquez, G. B., Militello, V., Leone, M., and Cupane, A. (1998) Properties of human hemoglobins with increased polarity in the α- or β-heme pocket. Carbonmonoxy derivatives. *J. Biol. Chem.* **273,** 23740–23749
9. Mathews, A. J., Olson, J. S., Renaud, J. P., Tame, J., and Nagai, K. (1991) The assignment of carbon monoxide association rate constants to the α and β subunits in native and mutant human deoxyhemoglobin tetramers. *J. Biol. Chem.* **266,** 21631–21639
10. Mathews, A. J., Rohlfs, R. J., Olson, J. S., Tame, J., Renaud, J. P., and Nagai, K. (1989) The effects of E7 and E11 mutations on the kinetics of ligand binding to R state human hemoglobin. *J. Biol. Chem.* **264,** 16573–16583
11. Nagai, K., Luisi, B., Shih, D., Miyazaki, G., Imai, K., Poyart, C., De Young, A., Kwiatkowsky, L., Noble, R. W., and Lin, S. H. (1987) Distal residues in the oxygen binding site of haemoglobin studied by protein engineering. *Nature* **329,** 858–860
12. Zhao, X., Vyas, K., Nguyen, B. D., Rajarathnam, K., La Mar, G. N., Li, T., Phillips, G. N., Jr., Eich, R. F., Olson, J. S., and Ling, J. (1995) A double mutant of sperm whale myoglobin mimics the structure and function of elephant myoglobin. *J. Biol. Chem.* **270,** 20763–20774
13. Jeong, S. T., Ho, N. T., Hendrich, M. P., and Ho, C. (1999) Recombinant hemoglobin(α29 leucine → phenylalanine, α96 valine → tryptophan, β108 asparagine → lysine) exhibits low oxygen affinity and high cooperativity combined with resistance to autoxidation. *Biochemistry* **38,** 13433–13442
14. Weir, N., Maillett, D. H., Shen, T. J., and Ho, C. (2009) Auto-oxidation of human hemoglobin and the roles of distal heme pocket substitutions. *Biophys. J.* **96,** 558a
15. Wiltrout, M. E., Giovannelli, J. L., Simplaceanu, V., Lukin, J. A., Ho, N. T., and Ho, C. (2005) A biophysical investigation of recombinant hemoglobins with aromatic B10 mutations in the distal heme pockets. *Biochemistry* **44,** 7207–7217
16. Tsuruga, M., and Shikama, K. (1997) Biphasic nature in the autoxidation reaction of human oxyhemoglobin. *Biochim. Biophys. Acta* **1337,** 96–104
17. Wallace, W. J., Houtchens, R. A., Maxwell, J. C., and Caughey, W. S. (1982) Mechanism of autooxidation for hemoglobins and myoglobins. Promotion of superoxide production by protons and anions. *J. Biol. Chem.* **257,** 4966–4977
18. Jaffé, E. R. (1982) Enzymopenic hereditary methemoglobinemia. *Haematologia* **15,** 389–399
19. Macdonald, V. W. (1994) Measuring relative rates of hemoglobin oxidation and denaturation. *Methods Enzymol.* **231,** 480–490
20. Varnado, C. L., Mollan, T. L., Birukou, I., Smith, B. J., Henderson, D. P., and Olson, J. S. (2013) Development of recombinant hemoglobin-based oxygen carriers. *Antioxid. Redox Signal.* **18,** 2314–2328
21. Ackers, G. K., Johnson, M. L., Mills, F. C., Halvorson, H. R., and Shapiro, S. (1975) The linkage between oxygenation and subunit dissociation in human hemoglobin. Consequences for the analysis of oxygenation curves. *Biochemistry* **14,** 5128–5134
22. Rother, R. P., Bell, L., Hillmen, P., and Gladwin, M. T. (2005) The clinical sequelae of intravascular hemolysis and extracellular plasma hemoglobin. A novel mechanism of human disease. *JAMA* **293,** 1653–1662
23. Chatterjee, R., Welty, E. V., Walder, R. Y., Pruitt, S. L., Rogers, P. H., Arnone, A., and Walder, J. A. (1986) Isolation and characterization of a new hemoglobin derivative cross-linked between the α-chains (lysine 99-α-1 → lysine 99-α-2). *J. Biol. Chem.* **261,** 9929–9937
24. Sehgal, L. R., Gould, S. A., Rosen, A. L., Sehgal, H. L., and Moss, G. S. (1984) Polymerized pyridoxylated hemoglobin. A red cell substitute with normal oxygen capacity. *Surgery* **95,** 433–438
25. Fitzgerald, M. C., Chan, J. Y., Ross, A. W., Liew, S. M., Butt, W. W., Baguley, D., Salem, H. H., Russ, M. K., Deasy, C., Martin, K. E., Mathew, J. K., and Rosenfeld, J. V. (2011) A synthetic haemoglobin-based oxygen carrier and the reversal of cardiac hypoxia secondary to severe anaemia following trauma. *Med. J. Aust.* **194,** 471–473
26. Natanson, C., Kern, S. J., Lurie, P., Banks, S. M., and Wolfe, S. M. (2008) Cell-free hemoglobin-based blood substitutes and risk of myocardial infarction and death. A meta-analysis. *JAMA* **299,** 2304–2312
27. Looker, D., Abbott-Brown, D., Cozart, P., Durfee, S., Hoffman, S., Mathews, A. J., Miller-Roehrich, J., Shoemaker, S., Trimble, S., and Fermi, G. (1992) A human recombinant haemoglobin designed for use as a blood substitute. *Nature* **356,** 258–260
28. Nagai, K., Perutz, M. F., and Poyart, C. (1985) Oxygen binding properties of human mutant hemoglobins synthesized in *Escherichia coli*. *Proc. Natl. Acad. Sci. U.S.A.* **82,** 7252–7255
29. Shen, T. J., Ho, N. T., Simplaceanu, V., Zou, M., Green, B. N., Tam, M. F., and Ho, C. (1993) Production of unmodified human adult hemoglobin in *Escherichia coli*. *Proc. Natl. Acad. Sci. U.S.A.* **90,** 8108–8112
30. Shen, T. J., Ho, N. T., Zou, M., Sun, D. P., Cottam, P. F., Simplaceanu, V., Tam, M. F., Bell, D. A., Jr., and Ho, C. (1997) Production of human normal adult and fetal hemoglobins in *Escherichia coli*. *Protein Eng.* **10,** 1085–1097
31. Maillett, D. H. (2003) *Engineering Hemoglobins and Myoglobins for Efficient O_2 Transport.* Ph.D. thesis, Rice University
32. Olson, J. S., Eich, R. F., Smith, L. P., Warren, J. J., and Knowles, B. C. (1997) Protein engineering strategies for designing more stable hemoglobin-based blood substitutes. *Artif. Cells Blood Substit. Immobil. Biotechnol.* **25,** 227–241
33. Brillet, T., Marden, M. C., Yeh, J. I., Shen, T. J., Ho, N. T., Kettering, R., Du, S., Vasseur, C., Domingues-Hamdi, E., Ho, C., and Baudin-Creuza, V. (2012) Interaction of haptoglobin with hemoglobin octamers based on the mutation αAsn78Cys or βGly83Cys. *Am. J. Mol. Biol.* **2,** 1–10
34. Wu, X., Ho, N. T., Shen, T. J., Vagni, V., Shellington, D. K., Janesko-Feldman, K., Tam, T. C. S., Tam, M. F., Kochanek, P. M., and Ho, C. (2013) Recombinant octameric hemoglobins as resuscitation fluids in a murine model of traumatic brain injury plus hemorrhagic shock. In *Hemoglobin Based Oxygen Carriers as Red Blood Cell Substitutes and Oxygen Therapeutics* (Kim, H. W., and Greenburg, A. G., eds) Springer, Berlin, Germany, in press
35. Russu, I. M., Lin, A. K., Ferro-Dosch, S., and Ho, C. (1984) A proton nuclear magnetic resonance investigation of human hemoglobin-A_2. Implications on the intermolecular contacts in sickle hemoglobin fibers and on the Bohr Effect of human normal adult hemoglobin. *Biochim. Biophys. Acta* **785,** 123–131
36. Hayashi, A., Suzuki, T., and Shin, M. (1973) An enzymic reduction system for metmyoglobin and methemoglobin and its application to functional studies of oxygen carriers. *Biochim. Biophys. Acta* **310,** 309–316
37. Plateau, P., and Gueron, M. (1982) Exchangeable proton Nmr without base-line distortion, using new strong-pulse sequences. *J. Am. Chem. Soc.* **104,** 7310–7311
38. Benesch, R. E., Benesch, R., and Yung, S. (1973) Equations for the spectrophotometric analysis of hemoglobin mixtures. *Anal. Biochem.* **55,** 245–248

39. Winterbourn, C. C., McGrath, B. M., and Carrell, R. W. (1976) Reactions involving superoxide and normal and unstable haemoglobins. *Biochem. J.* **155,** 493–502
40. Brancaccio, A., Cutruzzolá, F., Allocatelli, C. T., Brunori, M., Smerdon, S. J., Wilkinson, A. J., Dou, Y., Keenan, D., Ikeda-Saito, M., and Brantley, R. E., Jr. (1994) Structural factors governing azide and cyanide binding to mammalian metmyoglobins. *J. Biol. Chem.* **269,** 13843–13853
41. Ho, C. (1992) Proton nuclear magnetic resonance studies on hemoglobin-cooperative interactions and partially ligated intermediates. *Adv. Protein Chem.* **43,** 153–312
42. Chang, C. K., Simplaceanu, V., and Ho, C. (2002) Effects of amino acid substitutions at β131 on the structure and properties of hemoglobin. Evidence for communication between $\alpha_1\beta_1$- and $\alpha_1\beta_2$-subunit interfaces. *Biochemistry* **41,** 5644–5655
43. Russu, I. M., Ho, N. T., and Ho, C. (1987) A proton nuclear Overhauser effect investigation of the subunit interfaces in human normal adult hemoglobin. *Biochim. Biophys. Acta* **914,** 40–48
44. Simplaceanu, V., Lukin, J. A., Fang, T. Y., Zou, M., Ho, N. T., and Ho, C. (2000) Chain-selective isotopic labeling for NMR studies of large multimeric proteins. Application to hemoglobin. *Biophys. J.* **79,** 1146–1154
45. Fang, T. Y., Simplaceanu, V., Tsai, C. H., Ho, N. T., and Ho, C. (2000) An additional H-bond in the $\alpha_1\beta_2$ interface as the structural basis for the low oxygen affinity and high cooperativity of a novel recombinant hemoglobin (βL105W). *Biochemistry* **39,** 13708–13718
46. Dalvit, C., and Ho, C. (1985) Proton nuclear Overhauser effect investigation of the heme pockets in ligated hemoglobin. Conformational differences between oxy and carbonmonoxy forms. *Biochemistry* **24,** 3398–3407
47. Lindstrom, T. R., Norén, I. B., Charache, S., Lehmann, H., and Ho, C. (1972) Nuclear magnetic resonance studies of hemoglobins. 7. Tertiary structure around ligand binding-site in carbonmonoxyhemoglobin. *Biochemistry* **11,** 1677–1681
48. La Mar, G. N., Nagai, K., Jue, T., Budd, D. L., Gersonde, K., Sick, H., Kagimoto, T., Hayashi, A., and Taketa, F. (1980) Assignment of proximal histidyl imidazole exchangeable proton NMR resonances to individual subunits in hemoglobins A, Boston, Iwate, and Milwaukee. *Biochem. Biophys. Res. Commun.* **96,** 1172–1177
49. Takahashi, S., Lin, A. K., and Ho, C. (1980) Proton nuclear magnetic esonance studies of hemoglobin-M-Boston (α58E7 His → Tyr) and hemoglobin-M-Milwaukee (β67E11 Val → Glu). Spectral assignments of hyperfine-shifted proton resonances and of proximal histidine (E7) NH resonances to the α-chains and β-chains of normal human adult hemoglobin. *Biochemistry* **19,** 5196–5202
50. Fung, L. W., and Ho, C. (1975) Proton nuclear magnetic-resonance study of quaternary structure of human hemoglobins in water. *Biochemistry* **14,** 2526–2535
51. Ishimori, K., Imai, K., Miyazaki, G., Kitagawa, T., Wada, Y., Morimoto, H., and Morishima, I. (1992) Site-directed mutagenesis in hemoglobin. Functional and structural role of inter- and intrasubunit hydrogen bonds as studied with 37 β and 145 β mutations. *Biochemistry* **31,** 3256–3264
52. Birukou, I., Schweers, R. L., and Olson, J. S. (2010) Distal histidine stabilizes bound O_2 and acts as a gate for ligand entry in both subunits of adult human hemoglobin. *J. Biol. Chem.* **285,** 8840–8854
53. Yuan, Y., Simplaceanu, V., Ho, N. T., and Ho, C. (2010) An investigation of the distal histidyl hydrogen bonds in oxyhemoglobin. Effects of temperature, pH, and inositol hexaphosphate. *Biochemistry* **49,** 10606–10615
54. Birukou, I., Soman, J., and Olson, J. S. (2011) Blocking the gate to ligand entry in human hemoglobin. *J. Biol. Chem.* **286,** 10515–10529
55. Doherty, D. H., Doyle, M. P., Curry, S. R., Vali, R. J., Fattor, T. J., Olson, J. S., and Lemon, D. D. (1998) Rate of reaction with nitric oxide determines the hypertensive effect of cell-free hemoglobin. *Nat. Biotechnol.* **16,** 672–676
56. Fermi, G., Perutz, M. F., Shaanan, B., and Fourme, R. (1984) The crystal structure of human deoxyhaemoglobin at 1.74 Å resolution. *J. Mol. Biol.* **175,** 159–174
57. Park, S.-Y., Yokoyama, T., Shibayama, N., Shiro, Y., and Tame, J. R. (2006) 1.25 Å resolution crystal structures of human haemoglobin in the oxy, deoxy, and carbonmonoxy forms. *J. Mol. Biol.* **360,** 690–701
58. Barrick, D., Ho, N. T., Simplaceanu, V., and Ho, C. (2001) Distal ligand reactivity and quaternary structure studies of proximally detached hemoglobins. *Biochemistry* **40,** 3780–3795
59. Tame, J., Shih, D. T., Pagnier, J., Fermi, G., and Nagai, K. (1991) Functional role of the distal valine (E11) residue of α subunits in human haemoglobin. *J. Mol. Biol.* **218,** 761–767
60. Tucker, P. W., Phillips, S. E., Perutz, M. F., Houtchens, R., and Caughey, W. S. (1978) Structure of hemoglobins Zurich [His E7(63) β→Arg] and Sydney [Val E11(67) β→Ala] and role of distal residues in ligand binding. *Proc. Natl. Acad. Sci. U.S.A.* **75,** 1076–1080
61. Quillin, M. L., Li, T., Olson, J. S., Phillips, G. N., Jr., Dou, Y., Ikeda-Saito, M., Regan, R., Carlson, M., Gibson, Q. H., and Li, H. (1995) Structural and functional effects of apolar mutations of the distal valine in myoglobin. *J. Mol. Biol.* **245,** 416–436
62. Scott, E. E., Gibson, Q. H., and Olson, J. S. (2001) Mapping the pathways for O_2 entry into and exit from myoglobin. *J. Biol. Chem.* **276,** 5177–5188
63. Eaton, J. W., Skelton, T. D., and Berger, E. (1974) Survival at extreme altitude. Protective effect of increased hemoglobin-oxygen affinity. *Science* **183,** 743–744
64. Storz, J. F., Runck, A. M., Moriyama, H., Weber, R. E., and Fago, A. (2010) Genetic differences in hemoglobin function between highland and lowland deer mice. *J. Exp. Biol.* **213,** 2565–2574
65. Cole, R. H., Vandegriff, K. D., Szeri, A. J., Savaş, O., Baker, D. A., and Winslow, R. M. (2007) A quantitative framework for the design of acellular hemoglobins as blood substitutes. Implications of dynamic flow conditions. *Biophys. Chem.* **128,** 63–74